Paramagnetic Smectic Liquid Crystals: Synthesis and Properties of Bis(*N*-aryl-4-[(4′-decyloxy)benzyloxy]salicylaldimine)copper(II) and Oxovanadium(IV)

E. Campillos,[†] M. Marcos,*,[†] J. L. Serrano,[†] J. Barberá,[†] P. J. Alonso,[‡] and J. I. Martínez[‡]

Química Orgánica and Espectroscopía de Sólidos, Instituto de Ciencia de Materiales de Aragón, Facultad de Ciencias, Universidad de Zaragoza-C.S.I.C., 50009-Zaragoza, Spain

Received May 19, 1993. Revised Manuscript Received July 26, 1993[⊗]

The synthesis and characterization (by optical microscopy, differential scanning calorimetry (DSC), X-ray diffraction and electron paramagnetic resonance (EPR)) of two new series of low molecular weight paramagnetic complexes with copper atoms and oxovanadium groups derived from *N*-aryl-4-[(4′-decyloxy)benzyloxy]salicylaldimine are reported. These complexes form paramagnetic smectic mesophases (S_C and/or S_A). The X-ray diffraction patterns taken in the smectic A phase with oriented samples indicate a positive anisotropy of the magnetic susceptibility for both kinds of complex. The EPR spectra recorded at variable temperature indicate that in the smectic phase an exchange interaction remains in the copper(II) complexes and a restricted rotation of molecules takes place in both kinds of complex. The liquid-crystalline properties of the ligands are also discussed.

Introduction

The synthesis of metal-containing liquid crystals (metallomesogens) has increased considerably over the past few years due to the special combination of liquid-crystalline properties and the presence of a transition metal in the structure of the molecules which can give rise to unusual electrooptical and magnetic properties.[1]

Metal complexes of Schiff bases have played an important part in the development of metallomesogens as can be seen from the large number of publications that have appeared in the literature.[2,3] The particular advantage of the salicylaldimine ligand system is the considerable flexibility of the synthetic procedure which has allowed the preparation of a wide variety of complexes whose properties are strongly dependent on the ligand structure and on the metal used.[4] However, little is known about the relationship between the molecular structure and the mesophase behavior of these compounds. Recently, we have described the synthesis and mesogenic properties of Schiff base complexes of copper, nickel and oxovanadium derived from (*N*-aryl or alkyl-4-(4′-decyloxy)benzoyloxy)salicylaldimine[5-8] and copper complexes derived from *N*-aryl-4-alkoxysalicylaldimine.[9] According to the number and the position of the aromatic ring in the ligand and the metal atom, the mesogenic behavior and the magnetic properties of these complexes are very different. For example, the copper complexes show nematic or smectic properties, and negative or positive anisotropy of the magnetic susceptibility ($\Delta\chi$) depending on their structures.[10-14] The (*N*-(4′-*n*-alkoxyphenyl)-4-*n*-alkoxysalicylaldimine)copper(II) derivatives (series I, Figure 1) exhibit smectic A (S_A) and smectic C (S_C) mesophases, the (*N*-n-alkyl-4-(4′-*n*-decyloxybenzoyloxy)salicylaldimine)copper(II) complexes (series II, Figure 1) exhibit nematic (N) mesophase (and a smectic C mesophase for the *N*-methyl derivative) and both kinds of complex show negative $\Delta\chi$.[10,11,13] On the other hand, (*N*-(4″-*n*-alkoxyphenyl)-4-(4′-*n*-decyloxybenzoyloxy)salicylaldimine)copper(II) derivatives (series III, Figure 1) exhibit nematic and smectic C mesophases and a $\Delta\chi$ positive.[12,13]

To improve our knowledge of the relationship between molecular structure–mesogenic properties and molecular structure–magnetic behavior, we will analyze in this paper the results of the synthetic and mesogenic studies and the EPR and X-ray diffraction characterization of two families of copper(II) and oxovanadium(IV) complexes derived from a new type of Schiff base: *N*-(4″-*n*-alkoxyphenyl)-4-(4′-*n*-decyloxybenzyloxy)salicylaldimine with a general structure ML_2.

The $-CH_2O-$ link plays an important role in breaking the conjugation between the two aromatic rings but keeps

---

[†] Química Orgánica.

[‡] Espectroscopía de Sólidos.

[⊗] Abstract published in *Advance ACS Abstracts*, September 1, 1993.

(1) Piechocki, C.; Simon, J. *Nouv. J. Chim.* **1985**, *9*, 159.

(2) Giroud-Godquin, A. M.; Maitlis, P. M. *Angew. Chem., Int. Ed. Engl.* **1991**, *30*, 375.

(3) Espinet, P.; Esteruelas, M. A.; Oro, L. A.; Serrano, J. L.; Sola, E. *Coord. Chem. Rev.* **1992**, *117*, 215.

(4) Holm, R. H.; O'Connor, M. J. *Prog. Inorg. Chem.* **1971**, *14*, 477.

(5) Marcos, M.; Romero, P.; Serrano, J. L.; Barberá, J.; Levelut, A. M. *Liq. Cryst.* **1990**, *7*, 251.

(6) Marcos, M.; Romero, P.; Serrano, J. L. *Chem. Mater.* **1990**, *2*, 495.

(7) Marcos, M.; Romero, P.; Serrano, J. L. *J. Chem. Soc., Chem. Commun.* **1989**, 1641.

(8) Serrano, J. L.; Romero, P.; Marcos, M.; Alonso, P. J. *J. Chem. Soc., Chem. Commun.* **1990**, 859.

(9) Marcos, M.; Romero, P.; Serrano, J. L.; Bueno, C.; Cabeza, J. A.; Oro, L. *Mol. Cryst. Liq. Cryst.* **1989**, *167*, 123.

(10) Bikchantaev, I. G.; Galimov, R. M.; Ovchinnikov, I. V. *Theor. Exp. Chem.* **1988**, *24*, 360.

(11) Levelut, A. M.; Ghedini, M.; Bartolino, R.; Nicoletta, F. P.; Rustichelli, F. *J. Phys. (Paris)* **1989**, *50*, 113.

(12) Borchers, B.; Haase, W. *Mol. Cryst. Liq. Cryst.* **1991**, *209*, 319.

(13) Barberá, J.; Levelut, A. M.; Marcos, M.; Romero, P.; Serrano, J. L. *Liq. Cryst.* **1991**, *10*, 119.

(14) Marcos, M.; Serrano, J. L. *Adv. Mater.* **1991**, *30*, 256.

0897-4756/93/2805-1518$04.00/0

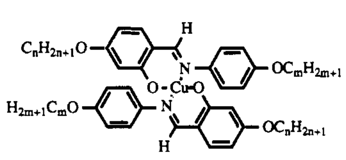

Series I S_A and S_C $\Delta\chi<0$

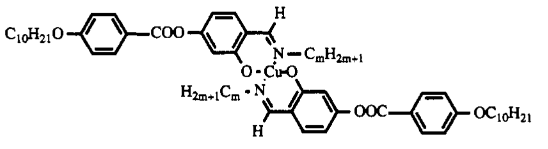

Series II N and S_C $\Delta\chi<0$

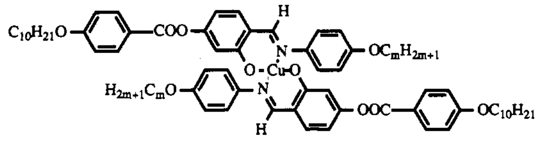

Series III N and S_C $\Delta\chi>0$

Figure 1. Homologous series of copper complexes: (a) Series I: (*N*-(4′-*n*-alkoxyphenyl)-4-*n*-alkoxysalicylaldimine)copper(II) complexes. (b) Series II: (*N*-*n*-alkyl-4-(4′-(*n*-decyloxy)benzoyloxy)salicylaldimine)copper(II) complexes. (c) Series III: (*N*-(4″-*n*-alkoxyphenyl)-4-(4′-*n*-decyloxybenzoyloxy)salicylaldimine)-copper(II) complexes.

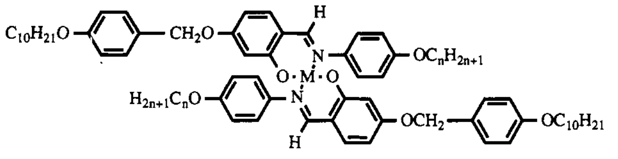

ML_2 M=Cu(II), VO(II) n= 1-10

the benzyl aromatic ring parallel to the main axis of the molecule. Both effects could be responsible for the mesogenic and magnetic properties of the complexes.

Experimental Section

Techniques. Microanalysis was performed with a Perkin-Elmer 240B microanalyzer. Infrared spectra for all the complexes were obtained using a Perkin-Elmer 1600 (FTIR) spectrophotometer in the 400–4000-cm^{-1} spectral range. Molecular weight determination was performed in $CHCl_3$ solution with a Knauer vapor pressure osmometer. ^1H and ^{13}C NMR spectra were recorded on a Varian Unity 300-Mz spectrometer in deuteriochloroform solutions. Mass spectroscopy (EI-MS) were performed using a VG Autospec spectrometer.

The textures of the mesophases were studied with an optical microscope (Nikon) equipped with polarized light, a Mettler FP82 hot stage, and a Mettler central processor.

Measurements of transition temperatures were made using a Perkin-Elmer DSC-2 differential scanning calorimeter with a heating or cooling rate of 10 K/min. The apparatus was calibrated with indium (156.6 °C, 28.4 J/g) and tin (232.1 °C, 60.5 J/g).

Thermogravimetric analyses were obtained on a Perkin-Elmer TGS-2 equipped with a system 4 microprocessor controller at a heating rate of 10 K/min under nitrogen.

Oriented X-ray diffraction patterns were obtained in a homemade camera with a monochromatic Cu Kα (λ = 1.5418 Å) X-ray beam issued from a double-bent pyrolytic graphite monochromator. The samples, held in Lindemann glass capillaries (ϕ = 0.5 mm), were aligned by a magnetic field (1.7 T) perpendicular to the X-ray beam. The temperature of the sample was constant to within ±1 K. The diffraction pattern was collected on a photographic film. Powder X-ray diffraction patterns were obtained in a Guinier diffractometer (Huber 644) operating with a Cu Kα_1 (λ = 1.5405 Å) beam issued from a germanium monochromator. The samples were held in rotating Lindemann glass capillaries (ϕ = 0.5 mm) and heated with a variable-temperature attachment. The diffraction patterns were registered with a scintillation counter.

EPR measurements were taken with a E-112 Varian or a ESP380 Bruker spectrometer, working in X-band. For measurements above room temperature, the variable-temperature accessories E-265 from Varian or ER 4111 VT from Bruker were used, respectively. Powder samples were put into quartz tubes, and the temperature was monitored using a copper–constantan thermocouple attached to the tube. The error in temperature was estimated to be lower than 0.5 °C, and stability was better than 0.1 °C. For measuring frozen solutions an immersion quartz dewar filled with liquid nitrogen was used.

Synthesis. The general reaction pathway to the target ligands (L) and the complexes (ML_2) is shown in Scheme I.

Preparation of the Schiff Bases. The free ligands L were synthesized using a well-known method[15] by mixing an ethanolic solution of 5.7 mmol of the 4-(4′-decyloxybenzyloxy)salicylaldehyde (**6**) with 5.7 mmol of the appropriate amine **7** and 2 drops of acetic acid as a catalyst and purified by recrystallization from ethanol (yields 65–78%).

The Schiff bases L and the intermediates were investigated by a variety of spectral techniques, including IR, ^1H NMR, ^{13}C NMR, and mass spectrometry. The analyses showed that the structures of all of the materials were consistent with those expected.

Selected spectroscopic data for ligand with n = 8 as a representative example: ^1H NMR (300 MHz, $CDCl_3$) δ = 13.94 (s, 1H, O*H*), 8.48 (s, 1H, C*H*=N), 7.33 (d, J = 8.6 Hz, 2H, benzyl), 7.20 (d, J = 8.9 Hz, 2H, *N*-aryl), 6.91 (d, J = 9.0 Hz, 2H, *N*-aryl), 6.89 (d, J = 8.6 Hz, 2H, benzyl), 6.51 (dd, J = 8.5 Hz, J = 2.4 Hz, 1H, salicylidene), 7.23 (d, J = 8.5 Hz, 1H, salicylidene), 6.56 (d, J = 2.3 Hz, 1H, salicylidene), 4.99 (s, 2H, $-CH_2O-$), 3.94 (t, 2H, $-CH_2CH_2O-$), 3.95 (t, 2H, $-CH_2CH_2O-$), 1.70–1.83 (m, 4H, CH_2 groups), 1.20–1.50 (m, 23H, CH_2 groups) 0.84–0.89 (m, 6H, 2 CH_3 groups); ^{13}C NMR (300 MHz, $CDCl_3$): 163.66, 162.79 (2 aromatic carbons), 159.40 (1C, CH=N), 159.17, 158.01, 141.13, 133.11, 129.31, 128.10, 121.96, 115.14, 114.62, 113.35, 107.57, 102.02 (16 aromatic carbons), 69.93 (1C, aryl-CH_2O-aryl), 68.32, 68.05 (2C, $C_9H_{19}CH_2O$-aryl, aryl-OCH_2-C_7H_{15}), 31.88, 31.80, 29.56, 29.54, 29.45, 29.38, 29.35, 29.30, 29.25, 29.23, 26.08, 26.02, 22.66, 22.65, (14C, CH_2 groups), 14.10 (2C, 2 CH_3); IR (Nujol, cm^{-1}) 1628 (C=N); MS (m/z) 587, 247, 107.

Synthesis of the Aldehyde 6. 4-(4′-Decyloxybenzyloxy)-salicylaldehyde (**6**) was obtained by etherification of 2,4-dihydroxybenzaldehyde (**5**, 18 mmol) with 4-decyloxybenzyl iodide (**4**, 18 mmol) in acetone as a solvent and $KHCO_3$ as a base following a method described previously.[16] The product was purified by flash chromatography using hexane/ethyl acetate (96/4) as an eluent (yield 45%), mp 76 °C; ^1H NMR (300 MHz, $CDCl_3$) δ 11.45 (s, 1H, O*H*), 9.68 (s, 1H, C*H*O), 7.41 (d, J = 8.5 Hz, 1H, salicylaldehyde), 7.31 (d, J = 8.6 Hz, 2H, benzyl), 6.89 (d, J = 8.6 Hz, 2H, benzyl), 6.58 (dd, J = 8.5, 2.3 Hz, 1H, salicylaldehyde), 6.49 (d, J = 2.3 Hz, 1H, salicylaldehyde), 5.00 (s, 2H, CH_2O), 3.94 (t, 2H, CH_2CH_2–O), 1.25–1.82 (m, 16H, CH_2 groups), 0.87 (t, 3H, CH_3); ^{13}C NMR (300 MHz, $CDCl_3$): 194.37 (CHO), 166.00, 164.45, 159.36, 135.23, 129.36, 127.33, 115.21, 114.69, 108.99, 101.54 (12 aromatic carbons), 70.29 (1C, aryl-CH_2O-aryl), 68.07 (1C, $C_9H_{19}CH_2O$-aryl), 31.87, 29.56, 29.54, 29.36, 29.30, 29.20, 26.01, 22.66 (8C, CH_2 groups), 14.10 (1C, CH_3); IR (nujol, cm^{-1}) 1643 (CHO).

Preparation of 4-Decyloxybenzyl Iodide (4). It was synthesized following a method described in the literature.[17] 4-Decyloxybenzyl alcohol (1 mol) was dissolved in toluene, and 1.3 mol of chlorodiphenylphosphine and 2.2 mol of imidazol were added under N_2 atmosphere. After 5 min, 1.3 mol of iodine dissolved in toluene was added dropwise by syringe to this solution; the reaction was stirred in darkness for 20 min, then washed with

---

(15) Keller, P.; Liebert, L. *Solid State Phys. Suppl.* **1978**, *14*, 19.

(16) Artigas, M.; Marcos, M.; Melendez, M.; Serrano, J. L. *Mol. Cryst. Liq. Cryst.* **1985**, *130*, 337.

(17) Classon, B.; Lin, Z.; Salmelsson, B. *J. Org. Chem.* **1988**, *53*, 6126.

Scheme I

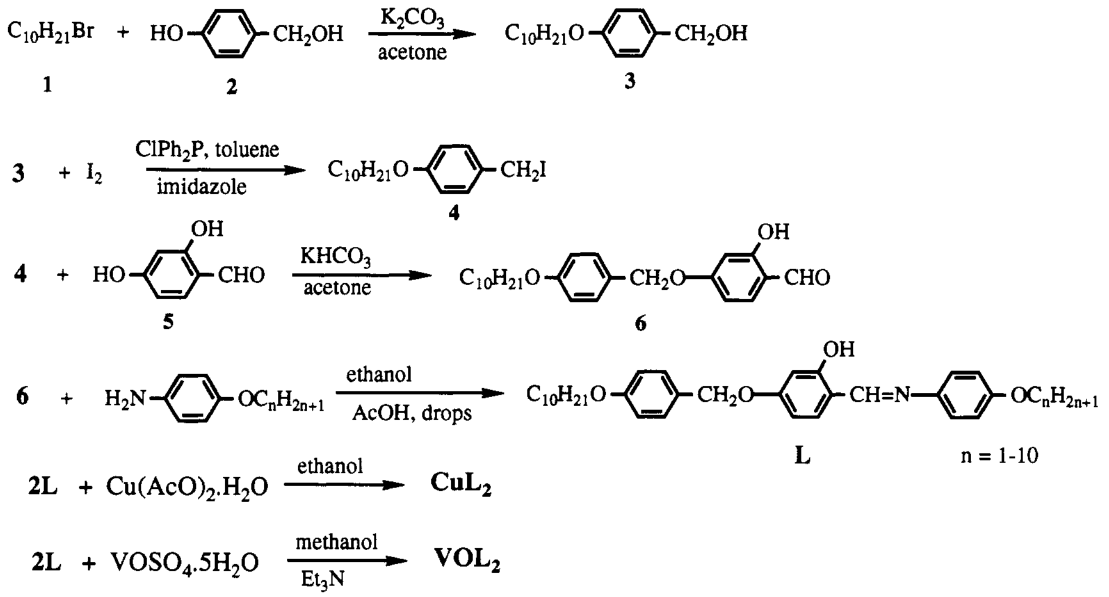

saturated aqueous sodium carbonate, saturated aqueous sodium sulfate and water, and dried over magnesium sulfate. The solvent was evaporated off, and compound 4 obtained was used without further purification (yield 95%).

4-Decyloxybenzyl alcohol (*3*) was obtained by O-alkylation of 50 mmol of 4-hydroxybenzyl alcohol (**2**) with 55 mmol of decyl bromide in acetone as a solvent and 55 mmol of K_2CO_3 as a base following the Williamson method.[18] Compound 3 was obtained after recrystallized from hexane (yield 60%), mp 59 °C. ^1H NMR (300 MHz, $CDCl_3$) δ 7.26 (d, J = 8.6 Hz, 2H, benzyl), 6.87 (d, J = 8.6 Hz, 2H, benzyl), 4.59 (s, 2H, CH_2OH), 3.93 (t, 2H, CH_2CH_2–O), 1.53 (s, br, 1H, CH_2OH), 1.20–1.81 (m, 16H, CH_2 groups), 0.86 (t, 3H, CH_3); ^{13}C NMR (300 MHz, $CDCl_3$) 158.78, 132.88, 128.62, 114.54 (6 aromatic carbons), 68.06 (1C, $-CH_2O-$), 65.06 (1C, $-CH_2-OH$), 31.89, 29.57, 29.55, 29.39, 29.31, 29.25, 26.02, 22.67 (8C, CH_2 groups), 14.11 (1C, CH_3); IR (Nujol, cm^{-1}) 3319, 3216 (OH).

Preparation of the Metal Complexes. The synthesis of copper(II) complexes was carried out as described previously,[6] by addition of an ethanolic solution (20 mL) containing copper(II) acetate ($Cu(OAc)_2{\cdot}H_2O$) (1 mmol) to a hot solution of the appropriate imine (2 mmol) in ethanol (50 mL). Oxovanadium(IV) complexes were synthesized by addition of a methanolic solution (20 mL) containing vanadium(IV) oxide sulfate ($VOSO_4{\cdot}5H_2O$) (1 mmol) in the presence of triethylamine to a hot solution of the appropriate imine (2 mmol) in methanol (50 mL).[19] In both cases the solution was refluxed for 1–2 h. After cooling, the precipitate was collected by filtration and recrystalized from a mixture of ethyl acetate and ethanol (1:3). The crystals are green for the oxovanadium complexes and brown for the copper complexes.

Elemental analysis, molecular weights, and yields are gathered in Table I.

Results and Discussion

Synthesis and Characterization. The ligands are prepared using a typical procedure. 4-(Decyloxy)benzyl alcohol was converted into 4-(decyloxy)benzyl iodide at room temperature using chlorodiphenylphosphine, iodine, and imidazole in stoichiometric amounts which react with 2,4-dihydroxybenzaldehyde using the Williamson method and the 4-(4′-(decyloxy)benzyloxy)salicylaldehyde so formed gave the Schiff bases (L) by treatment with the appropriate 4-alkoxyaniline.

Table I. Analytical Data, Molecular Weights, and Yields for Complexes (Calculated Values in Parentheses)

n	M	C %	H %	N %	mol wt	yield %
1	Cu	71.8 (71.5)	7.8 (7.4)	2.5 (2.7)	1020 (1040.8)	74
2	Cu	71.3 (71.9)	7.9 (7.5)	2.5 (2.6)	1095 (1068.9)	82
3	Cu	72.4 (72.3)	8.0 (7.7)	2.5 (2.5)	1040 (1096.9)	71
4	Cu	72.4 (72.6)	8.2 (7.9)	2.2 (2.5)	1090 (1125.0)	74
5	Cu	72.5 (72.9)	8.4 (8.0)	2.4 (2.4)	1160 (1153.0)	79
6	Cu	73.8 (73.2)	8.7 (8.2)	2.6 (2.4)	1195 (1181.1)	80
7	Cu	73.8 (73.5)	8.8 (8.3)	2.2 (2.3)	1270 (1209.2)	83
8	Cu	73.7 (73.8)	8.7 (8.5)	2.3 (2.3)	1270 (1237.2)	75
9	Cu	74.6 (74.0)	9.1 (8.6)	2.2 (2.2)	1240 (1265.3)	71
10	Cu	73.9 (74.3)	9.2 (8.7)	2.2 (2.2)	1265 (1293.3)	79
1	VO	71.8 (71.3)	7.8 (7.3)	2.7 (2.7)	1080 (1044.2)	69
2	VO	72.1 (71.7)	8.0 (7.5)	2.7 (2.7)	1105 (1072.3)	73
3	VO	72.4 (72.0)	8.1 (7.7)	2.6 (2.6)	1150 (1100.3)	65
4	VO	72.8 (72.4)	8.2 (7.9)	2.6 (2.5)	1100 (1128.4)	74
5	VO	73.1 (72.7)	8.4 (8.0)	2.6 (2.4)	1125 (1156.4)	75
6	VO	73.5 (73.0)	8.6 (8.2)	2.5 (2.4)	1200 (1184.5)	71
7	VO	73.8 (73.3)	8.6 (8.3)	2.3 (2.3)	1220 (1212.6)	68
8	VO	73.9 (73.6)	8.9 (8.5)	2.4 (2.3)	1220 (1240.6)	75
9	VO	74.2 (73.9)	9.0 (8.6)	2.3 (2.2)	1230 (1268.7)	70
10	VO	74.4 (74.1)	8.9 (8.7)	2.0 (2.2)	1340 (1296.7)	69

The copper complexes were prepared by reacting the appropriate imine with copper acetate monohydrate in warm ethanol. The oxovanadium complexes were prepared by reacting the appropriate imine with vanadyl sulfate pentahydrate and triethylamine in warm methanol. The complexes are soluble in chloroform and dichloromethane, partially soluble in ethyl acetate and acetone and insoluble in ethanol. The elemental analyses of the complexes are consistent with their proposed structures. Molecular weight determinations of the complexes in $CHCl_3$ solution show that they have a ratio of 2:1 ligand: metal, as expected (Table I).

The C═N stretching vibration in the ligands is located in the 1625–1628-cm^{-1} region and is shifted to lower wavenumbers (approximately 16 cm^{-1} for copper complexes and 12 cm^{-1} for oxovanadium complexes) upon chelation, indicating that the azomethine N atom is involved in metal–nitrogen bond formation. The oxovanadium complexes also exhibit a stretching band at around 980–974 cm^{-1}, assigned to ν(V═O) which is slightly shifted to higer wavenumbers (approximately 10 cm^{-1}) in the mesophase or isotropic liquid this suggests that these

---

[18] Marcos, M.; Melendez, M.; Serrano, J. L. *Mol. Cryst. Liq. Cryst.* 1983, *91*, 157.

[19] Farmer, R. L.; Urbach, F. L. *Inorg. Chem.* 1974, *13*, 587.

Table II. Optical, Thermal, and Thermodynamic Data[a] for the Ligands and Complexes

	ligands		copper complexes		oxovanadium complexes	
n	transition	*T* (°C) (kJ/mol)	transition	*T* (°C) (kJ/mol)	transition	*T* (°C) (kJ/mol)
1	C–N	125.4 (51.91)	C–S$_A$	156.2 (41.13)	C–C′	116.6 (13.62)
	N–I	168.7 (1.94)	S$_A$–I	195.8 (7.54)	C′–S$_A$	173.9 (8.82)
					S$_A$–I	193.2 (6.02)
2	C–S$_C$	118.1 (43.80)	C–S$_A$	161.8 (43.64)	C–C′	115.2 (18.05)
	S$_C$–N	153.2 (0.37)	S$_A$–I	226.0 (11.61)	C′–S$_A$	170.6 (5.74)
	N–I	185.1 (2.63)			S$_A$–I	217.3 (7.20)
3	C–S$_C$	113.9 (51.98)	C–S$_A$	165.1 (50.68)	C–C′	108.3 (34.29)
	S$_C$–N	167.6 (1.28)	S$_A$–I	223.4 (14.38)	C′–SA	164.0 (7.13)
	N–I	178.9 (4.00)			SA–I	211.0 (11.41)
4	C–S$_C$	107.3 (49.23)	C–S$_A$	154.7 (42.95)	C–C′	102.3 (34.48)
	S$_C$–N	180.5 (9.10)	S$_A$–I	230.0 (17.71)	C′–S$_A$	155.6 (4.67)
	N–I	183.5 (3.99)			S$_A$–I	206.7 (12.31)
5	C–S$_I$	99.1 (45.02)	C–S$_C$	160.5 (22.30)	C–C′	97.2 (10.49)
	S$_I$–S$_C$	111.0 (0.60)	S$_C$–S$_A$	177^b	C′–S$_A$	203.1 (32.05)
	S$_C$–I	181.0 (11.45)	S$_A$–I	227.6 (18.44)	S$_A$–I	236.9 (17.93)
6	C–S$_I$	96.2 (46.10)	C–S$_C$	160.3 (24.39)	C–C′	95.0 (18.02)
	S$_I$–S$_C$	110.9 (0.60)	S$_C$–S$_A$	180^b	C′–S$_C$	170.5 (32.05)
	S$_C$–I	181.6 (14.16)	S$_A$–I	225.8 (19.30)	S$_C$–S$_A$	184^b
					S$_A$–I	213.4 (17.97)
7	C–S$_I$	95.1 (58.16)	C–S$_C$	161.3 (23.65)	C–C′	91.3 (2.96)
	S$_I$–S$_C$	111.0 (0.60)	S$_C$–I	220.6 (19.95)	C′–S$_C$	182.4 (27.90)
	S$_C$–I	180.0 (14.16)			S$_C$–S$_A$	213^b
					S$_A$–I	225.7 (17.03)
8	C–S$_I$	90.9 (54.99)	C–S$_C$	158.5 (23.78)	C–C′	89.8 (13.85)
	S$_I$–S$_C$	111.3 (0.83)	S$_C$–I	217.6 (20.76)	C′–S$_C$	156.0 (14.42)
	S$_C$–I	180.4 (15.23)			S$_C$–I	211.0 (18.55)
9	C–S$_I$	97.1 (61.64)	C–S$_C$	153.9 (24.66)	C–C′	95.5 (2.81)
	S$_I$–S$_C$	111.7 (0.83)	S$_C$–I	212.0 (21.09)	C′–S$_C$	166.9 (26.97)
	S$_C$–I	180.0 (17.03)			S$_C$–I	212.5 (18.86)
10	C–S$_I$	103.6 (42.82)	C–S$_C$	141.0 (38.52)	C–C′	100.0 (11.32)
	S$_I$–S$_C$	111^b	S$_C$–I	210.0 (20.81)	C′–S$_C$	145.1 (20.65)
	S$_C$–I	174.9 (14.72)			S$_C$–I	207.4 (20.49)

[a] Data referred to the first DSC cycle (complexes partially decompose after the first heating cycle). [b] Microscopy data.

complexes have a monomeric structure.[19-21]

The thermal stability of the complexes was studied by thermogravimetric analysis, and none of the complexes shows a weight loss until 270 °C. However, we observed by optical microscopy that the complexes partially decompose after the complex has become isotropic and the second DSC scan differs from the first. For this reason first-scan DSC data were used.

Mesogenic Behavior. The optical, thermal, and thermodynamic data of the ligands and the complexes are gathered in Table II.

As can be observed, all the compounds synthesized, both ligands and complexes, exhibit mesogenic behavior. The introduction of a metal raises the transition temperatures, melting and clearing points.

The mesophases were assigned on the basis of their optical texture and in some cases confirmed by X-ray diffraction studies.

Ligands show nematic (N) phase, smectic C (S$_C$) mesophase and smectic I (S$_I$) phase (Figure 2). The nematic mesophase showed the marbled texture on heating and the schlieren texture on cooling. The smectic C mesophase is clearly identified on the cooling process by their typical schlieren and focal conic textures. These textures flash when the sample is subjected to mechanical stress and as a result of homogeneous texture appears. Typical transition bars are observed during the smectic C to nematic transition when the two mesophases appears. Formation of bâtonntes was observed when the smectic C phase appears from the isotropic liquid. The smectic I mesophase was identified by the schlieren texture obtained on cooling from the schlieren form of the smectic C mesophase. The nature of this mesophase together the smectic C phase were confirmed by X-ray diffraction studies. Powder patterns of a representative ligand of the series (*n* = 7) were registered at different temperatures. The pattern taken on the higher-temperature mesophse (at 120 °C) shows a small-angle sharp peak and large-angle diffuse scattering; this pattern is characteristic of a layered structure (periodicity 33.1 Å) with no order within the layers and supports the smectic C nature of the mesophase. The pattern taken on the lower temperature mesophase of the same ligand (at 100 °C) shows a sharpening of the large-angle scattering which transforms into an intense maximum. This, together with the optical textures, points to the smectic I nature of this mesophase. The measured interlayer periodicity is 33.5 Å and the

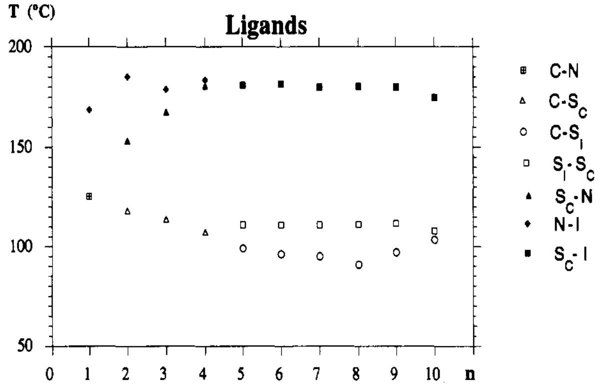

Figure 2. Plot of phase transition temperatures versus alkoxy chain length (*n*) for ligands.

---

(20) Pasquali, M.; Marchetti, F.; Floriani, C.; Merlino, S. *J. Chem. Soc., Dalton Trans.* **1977**, 139.

(21) Serrette, A.; Carroll, J.; Swager, T. M. *J. Am. Chem. Soc.* **1992**, *114*, 1887.

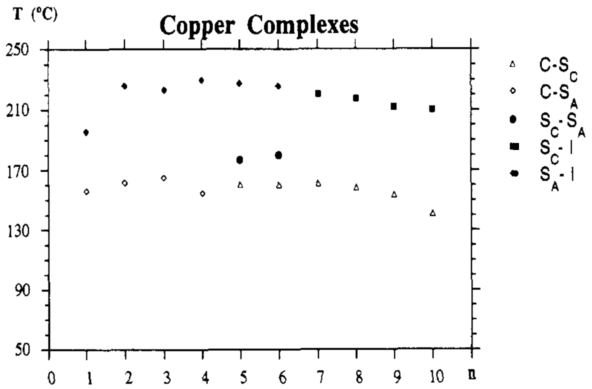

Figure 3. Plot of phase transition temperatures versus alkoxy chain length (n) for copper(II) complexes.

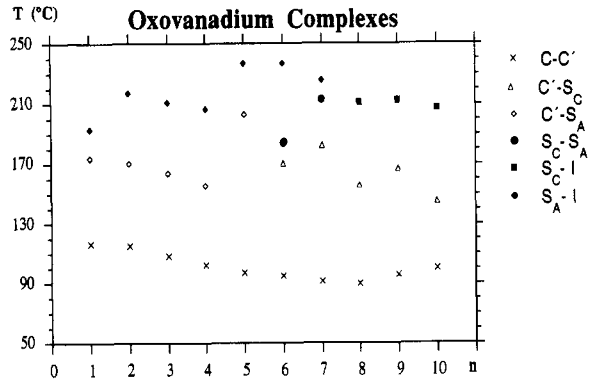

Figure 4. Plot of phase transition temperatures versus alkoxy chain length (n) for oxovanadium(IV) complexes.

intermolecular distance in the in-layer pseudohexagonal array is 5.13 Å.

The mesophases shown by the complexes (Figures 3 and 4) were identified as smectic C and smectic A (S_A). The optical textures are similar to those observed for classical rodlike organic compound. The S_A phase present in copper(II) (n = 1–6) and oxovanadium(IV) (n = 1–7) complexes was identified by its fan-shaped texture on cooling from the isotropic liquid which become homeotropic when the samples is submitted to mechanical stress. The S_C mesophase present in the copper(II) (n = 5–10) and oxovanadium(IV) (n = 6–10) complexes shows broken focal conic when was obtained on cooling the fan-shaped S_A phase. A pseudohomeotropic texture is obtained on applying mechanical stress to the sample. If the smectic C is formed on cooling the homeotropic spectic A texture a pseudohomeotropic texture is observed. Formation of bâtonntes was observed when the smectic C phase appears from the isotropic liquid (n = 7–10 for copper(II) complexes and n = 8–10 for oxovanadium(IV) complexes).

In addition to the fluid liquid-crystalline phases all oxovanadium complexes show at lower temperatures an additional birefringent more viscous phase. To investigate the nature of this phase, powder patterns were taken on the oxovanadium(IV) complexes where n = 2, 5, 9. Very complicated patterns were obtained with a great number of reflections which is not characteristic of any mesophase. This suggests that we are dealing with a three-dimensional crystal rather a mesophase, and thus we denoted it as C′ in Table II.

The copper complexes have slightly wider mesophase ranges than the oxovanadium complexes and the melting points are lower; however clearing points are similar (Table II). Whereas in copper complexes the transition temperatures do not change appreciably when the chain length is varied (Figure 3), in oxovanadium complexes an odd–even effect at the melting point is observed for compounds with terminal chain $n \geq 5$ (Figure 4).

Table III. Structural Characteristics of the Mesophases[a]

n	M	phase	d (Å)	D (Å)	l (Å)	$\Delta\chi$ (sign)
2	Cu	S_A	36.1	4.6	36	+
5	Cu[b]	S_A	37.1	4.6	40.5	+
		S_C	37.1	4.6		
9	Cu	S_C	34.7	4.6	45.5	[c]
2	VO	S_A	35.0	4.7	36	+
5	VO	S_A	35.0	4.7	40.5	+
9	VO	S_C	34.4	4.7	45.5	+

[a] d, layer periodicity in the smectic phase, D, intermolecular mean distance, l calculated molecular length of the ligands from Dreiding stereomodels, $\Delta\chi$ anisotropy of magnetic susceptibility for some copper and oxovanadium complexes. [b] Value estimated for the tilt angle in the S_C 6°. [c] The SC phase could not be aligned magnetically.

As far as the clearing enthalpy is concerned, there are differences between the ligands and the complexes; generally higher values are observed for the complexes than for the corresponding ligands when the transition type is the same and they are also higher in the copper complexes than in the oxovanadium complexes (for example, when n = 8 the S_C–I transition has a ΔH = 15.23 kJ/mol for the ligand, 20.76 kJ/mol for the copper complex, and 18.55 kJ/mol for the oxovanadium complex.

X-ray Diffraction Studies of Oriented Samples. An X-ray diffraction study has been made of the magnetically aligned monodomains of three complexes of copper and three complexes of oxovanadium where n = 2, 5, 9. They were studied in the smectic A and/or smectic C phases.

The structural characteristics of the mesophase, layer periodicity in the smectic phase (d), average intermolecular lateral distance (D), and sign of anisotropy of magnetic susceptibility ($\Delta\chi$) are gathered in Table III.

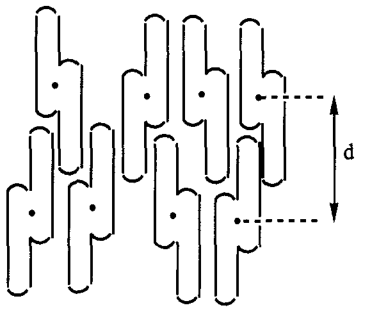

The diffraction patterns obtained show that the samples oriented well in the smectic A state and orientation was difficult in smectic C. As an example, the diffraction pattern of the S_A mesophase for the copper complex where n = 2 is shown in Figure 5.

The S_A patterns generally show a set of two (or three) sharp reflections in the long-angle region along the direction of alignment, with a Bragg distance ratio $1:{}^1/_2$ $({}^1/_3)$, characteristic of the smectic (lamellar) systems. From these reflections Bragg's law gives the layer periodicity d (see Table III). The wide-angle region exhibits a diffuse maximum split into two crescents concentrated in the equatorial plane (direction perpendicular to the director). This maximum gives a distance D of about 4.6–4.7 Å (see Table III) typically observed in classical calamitic liquid crystals.

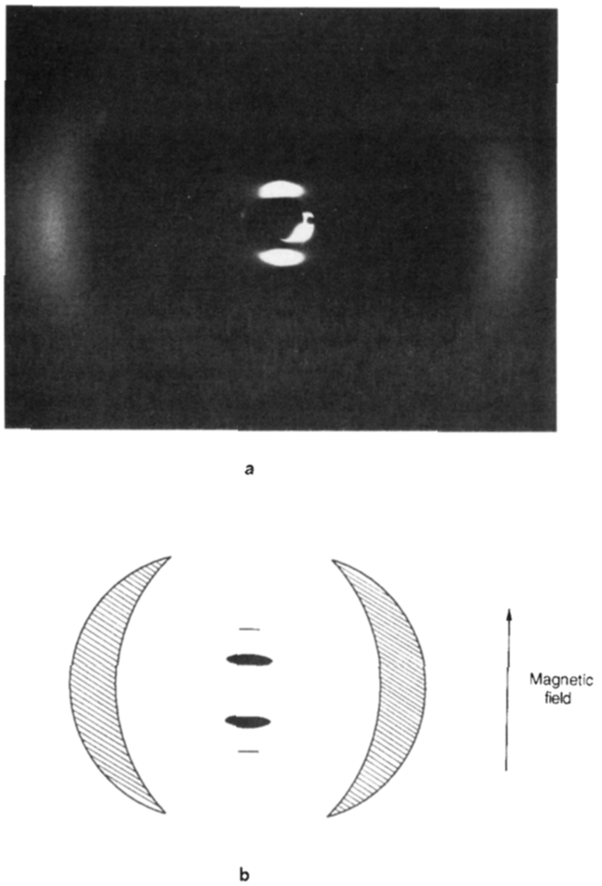

Figure 5. Diffraction pattern of the SA mesophase of the n = 2 copper complex. (a) X-ray photograph; (b) schematic representation.

The absence of scattering at middle angles in our compounds rules out the side-by-side local coupling of molecules observed in other copper salicylaldimine complexes[11] and in some palladium complexes[22] where a diffuse intensity corresponding to a distance of approximately 8.5 Å appears in the equatorial plane.

It can be noted in Table III that the layer thickness d is practically independent of the metal and of n (chain length of the amine part). By comparing the d values with the ligand lengths calculated from Dreiding stereomodels for an all-trans conformation (l) it can be seen that both values are similar for $n = 2$ (d = 36.1 Å for copper complex, d = 35.0 Å for VO; l = 36 Å), whereas d is smaller than l for $n = 5$ (d = 37.1 Å for Cu, d = 35.0 Å for VO; l = 40.5 Å) and $n = 9$ (d = 34.7 Å[23] for Cu, d = 34.4 Å for VO; l = 45.5 Å). The d values are in all cases much lower than the estimated length of the complexes (53 Å, calculated from Dreiding stereomodels for an all-trans conformation). These features are consistent with an interdigitated array of neighboring layers due to the peculiar shape of this kind of molecule. Thus, the interlayer spacing corresponds to the ligand length in the case of the $n = 2$ compound, and the d values is even smaller than the l value for $n = 5$ and $n = 9$ complexes; this can be explained by the conformational freedom of the chains in the smectic state, which leads to a shortening of the molecule length compared to that of the all-trans structure.

From the pattern it can be deduced that the main molecular axis orients with the applied magnetic field, which means that the anisotropy of the magnetic susceptibility $\Delta\chi$ is positive in these compounds. This result agrees with data obtained for copper and oxovanadium complexes derived from 4-(4′-(decyloxy)benzoyloxy)salicylidene-4″-alkoxyanilines[12,13] and differs from the data found with some analogous copper complexes described in the literature derived from 4-alkoxysalicylidene-4′-(alkyl or alkoxy)anilines[10,11] where the molecules orient with the main molecular axis perpendicular to the magnetic field and the material exhibits an anisotropy of the magnetic susceptibility negative.

The direction of alignment of the molecules by a magnetic field depends on the sign of the anisotropy of the magnetic susceptibility. In the case of paramagnetic metallorganic molecules like those considered in the present work there are two main contributions to $\Delta\chi$: the contribution of the paramagnetic entity due to the anisotropy of the g tensor and the contribution of the strong anisotropic diamagnetic susceptibility of the benzene rings. A compromise between them is responsible for the actual orientation of the whole molecule in the presence of a magnetic field. In the case of the vanadyl complexes the anisotropy of the paramagnetic contribution is small ($g_{\parallel} < g_{\perp}$), this favors the V–O bond being perpendicular to the magnetic field and the oxovanadium molecules orient with their main axis parallel to the magnetic field regardless the number of benzene rings. This behavior coincides with that previously reported in other VO metallomesogen compounds.[24]

On the other hand in the case of copper complexes $g_{\parallel} > g_{\perp}$ and the paramagnetic contribution to the magnetic susceptibility tends to orient the molecules perpendicular to the magnetic field in a opposite way that the diamagnetic contribution which depends on the number of benzene rings. This explains why the molecules with only four rings orient perpendicular to the magnetic field, while those with six aromatic ring tend to align their long axis along the external field.

EPR Studies. EPR spectroscopy has proved to be a useful tool for studying the mesomorphic behavior of paramagnetic metallomesogen compounds.[10,25–28] From these studies information about intermolecular exchange, molecular ordering, and dynamical effects associated with the molecular motion in the different phases can be obtained. Particularly in copper compounds strong exchange interactions have been found which remain even in fluid phases like smectic ones.[26] On the other hand Ghedini et al.[27] explain their results on the bases of the existence of some anisotropic molecular motions even in the room-temperature solid phases, but they exclude the existence of intermolecular exchange interactions. Finally Hoshino et al.[28] use the thermal evolution of the EPR spectrum for determining an Maier-Saupe-like parameter and their results show some discrepancies with the order parameter derived from NMR measurements.

---

(22) Espinet, P.; Perez, J.; Marcos, M.; Ros. M. B.; Serrano, J. L.; Barberá, J.; Levelut, A. M. *Organometallics* **1990**, *9*, 2028.

(23) In this case d corresponds to the S_C mesophase; so the tilt angle contributes also to the reduction of the d value.

(24) Alonso, P. J.; Sanjuán, M. L.; Romero, P.; Marcos, M.; Serrano, J. L. *J. Phys. Condens. Matter.* **1990**, *2*, 9173.

(25) Alonso, P. J.; Marcos, M.; Martínez, J. I.; Orera, V. M.; Sanjuán, M. L.; Serrano, J. L. *Liq. Cryst.* **1993**, *13*, 585.

(26) Eastman, M. P.; Horng, M.; Freiha, B.; Shew, K. W. *Liq. Cryst.* **1987**, *2*, 223.

(27) Ghedini, M.; Morrone, S.; Gatteschi, D.; Zanchini, C. *Chem. Mater.* **1991**, *3*, 752.

(28) Hoshino, N.; Kodama, A.; Shibuya, T.; Matsunaga, Y.; Miyajima, S. *Inorg. Chem.* **1991**, *30*, 3091.

With these ideas in mind we have undertaken an EPR study of the copper and oxovanadium compounds here reported (mainly with $n = 2, 5, 9$) measured at different temperatures above room temperatures. It has been found that the spectra do not depend on the aliphatic chain length n and that they undergo modifications when the phase transition takes place. However, no differences were observed between the spectra of the S_C and S_A phases. This confirms the paramagnetic character of the metalloorganic compounds. It is also noteworthy that if a sample is warmed to any temperature below the clearing point and then cooled to room temperature, its behavior in subsequent heating cycles is the same, but if it is carried to the isotropic phase an irreversible change is observed. This behavior also happens regardless of the aliphatic chain length (these results contrast with those reported by Ghedini et al.[27]). For all these reasons, we have restricted ourselves to reporting the EPR result of the $n = 9$ compounds. As will be seen, in all cases the spectra consists of broad lines and the hyperfine structure, if any, is hardly resolved. To get information about the electronic properties of the *isolated* molecules, we have also measured the EPR spectrum of solutions of our compounds in toluene. These solutions were frozen by immersion in liquid nitrogen, and the spectra were measured at this temperature. Under these conditions the resonance lines proved to be narrower, and a good resolution was observed because the intermetallic interactions decrease considerably. These spectra correspond to the isolated molecules and can be described with a standard axial spin Hamiltonian including a Zeeman and a hyperfine contribution ($I = {}^3/_2$ for Cu and $I = {}^7/_2$ for VO). The values for the spin Hamiltonian parameters which show the best agreement between the calculated and the observed spectrum turned out to be independent of the aliphatic chain and take the values $g_\parallel = 2.235 \pm 0.005$, $g_\perp = 2.050 \pm 0.005$, $A_\parallel = 500 \pm 10$ MHz, $A_\perp < 30$ MHz for copper compounds and $g_\parallel = 1.945 \pm 0.005$, $g_\perp = 1.978 \pm 0.005$, $A_\parallel = 500 \pm 10$ MHz, $A_\perp = 170$ MHz for the oxovanadium ones.

We will now turn our attention to the spectra in the condensed phases. In Figure 6 we show the EPR spectra of the copper(II) complex where $n = 9$. The top trace (Figure 6a) corresponds to the *as-received* sample measured at room temperature. It consists of two *features*, one in the low-field region with a *parallel* character and the other on the high-field side, which shows a *perpendicular* character. The resonance fields are in agreement with the g factors observed in the solutions (see above). No indications of a HF structure were found which indicates that an exchange interaction between the paramagnetic entities takes place. As commented in an early paper[25] the fact that the observed g factors coincide with those found for isolated molecules (see above) indicates that in the condensed phase the axis of the molecules remains practically parallel.

When the sample is warmed up to the smectic phase a change in its EPR spectrum is observed. A typical trace found in the smectic phase is given in Figure 6b and corresponds to a spectrum taken at 200 °C. It can be observed that the resonance lines broaden, while the anisotropy of the whole spectrum markedly decreases. As discussed elsewhere[25] two reasons can in principle be the cause of this effect: the freedom of motion in the smectic phase together with the exchange interaction between paramagnetic entities in adjacent molecules whose molecular axes are slightly tilted. This effect is confirmed by looking at the EPR spectrum of the frozen S_C phase (Figure 6c). In this situation the motional effects are eliminated, giving rise to a narrowing of the lines, whereas the exchange interaction between nonparallel molecules is retained, producing a partial averaging of the signal and destroying the HF structure.

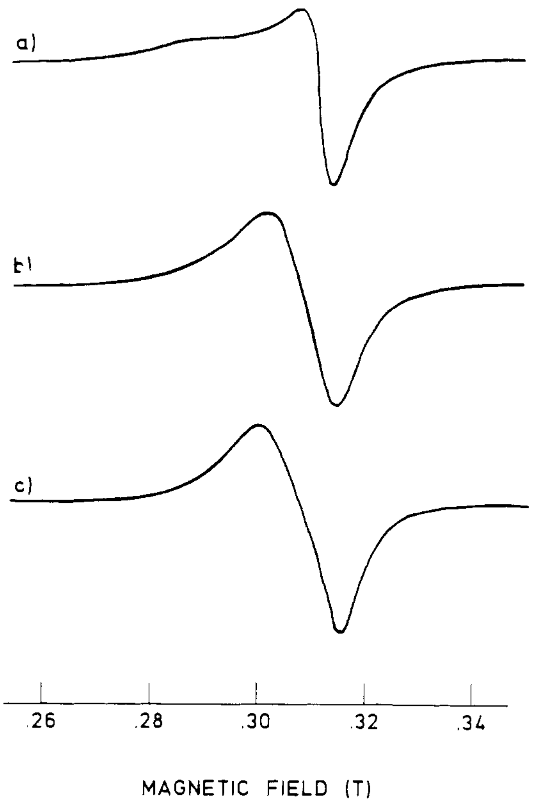

Figure 6. EPR spectra of the $n = 9$ copper compound. (a) As-received samples measured at room temperature. b) Measured at 200 °C; S_C phase. (c) Frozen S_c phase measured at room temperature.

The behavior of the oxovanadium compounds is a little more complicated but can be understood in a similar way. The room-temperature spectrum of a $n = 9$ *virgin* sample is given in Figure 7a. It consists of broad lines (peak-to-peak width of about 17 mT) without any clearly resolved structure except for some shoulders barely observed in the low field wing which, as we will see, correspond to the *parallel* HF structure. When the sample undergoes the C–C′ transition, small changes are observed in the EPR spectrum and the HF components begin to appear (see Figure 7b). They become clearly resolved when a fluid phase is reached: either a smectic C mesophase (Figure 7c) or an isotropic one (Figure 7d). It is also noteworthy that in these fluid phases the separation of the outermost lines decreases as the temperature increases.

The presence of the resolved HF structure indicates that in the oxovanadium complexes the exchange interaction, if any, is negligible, and so the thermal shift of the HF lines is attributed to a motion of the molecules around their molecular long axis (hindered rotation or libration) which takes place in the fluid phases and becomes more marked as the temperature is increased.

A discussion of this topic is outside the scope of the present paper and will be analyzed elsewhere. A preliminary discussion on this point has been recently present-

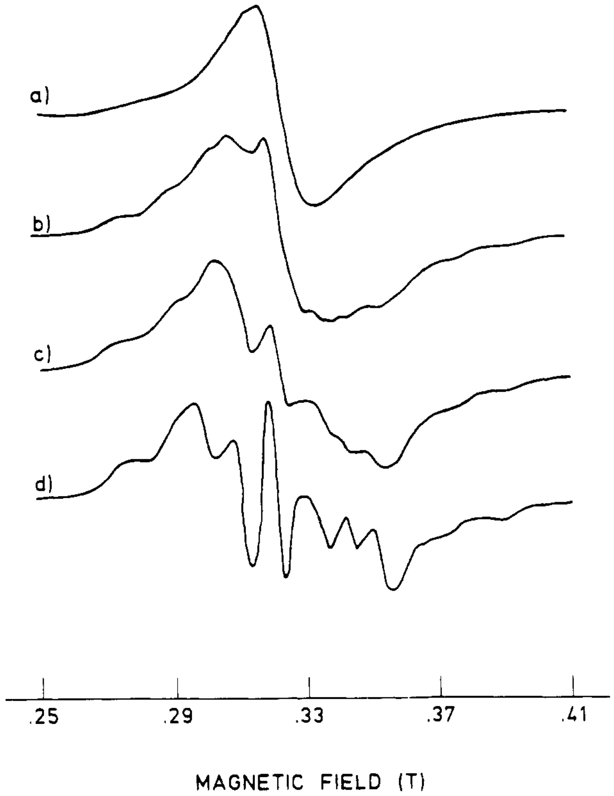

Figure 7. EPR spectra of the $n = 9$ oxovanadium compound. (a) As-received samples measured at room temperature. (b) Measured at 150 °C; C′ phase. (c) Measured at 170 °C; S_A phase. (d) Measured at 220 °C; isotropic phase.

ed.[29] In any case, the lack of the free rotation of the molecules can be understood as a consequence of their shape that is closer to a prismlike shape than to a rodlike shape and it is in agreement with the interdigitated packing of the molecules as can be seen in the X-ray diffraction studies.

Conclusions

Two main conclusions can be deduced from this study. As far as molecular structure–mesogenic behavior is concerned, all the complexes (copper and oxovanadium) show paramagnetic smectic behaviour (S_A and S_C) like the complexes derived from 4-alkoxysalicylaldimines (series I, Figure 1). In this case the $-CH_2O-$ group breaks the conjugation between the benzene rings, thus preventing an increase in the anisotropy of the electronic polarizability. It follows from this that the 4-(decyloxy)benzyl terminal group acts in the same way as an *n*-alkoxy terminal chain with regard to mesogenic properties.

On the other hand, both kinds of complex exhibit a positive anisotropy of magnetic susceptibility, which means that the main molecular axis orients with the magnetic field, as occurs with the complexes derived from *N*-(4″-*n*-alkoxyphenyl)-4-(4′-(decyloxy)benzoyloxy)salicylaldimines (series III, Figure 1). This means that the diamagnetic contribution of the benzyl ring is added to the diamagnetic contribution of the other aromatic rings of the molecule and predominates over the paramagnetic contribution due to the metal. In conclusion, we cay say that the number and geometrical position of the aromatic rings play an important role in the magnetic behavior regardless of electronic factors such as molecular conjugation.

Acknowledgment. This work was financed by the CICYT (Spain, projects No. MAT90-0813 and MAT90-0748). Thanks are due to the Ministerio de Educación y Ciencia for a grant to E.C. and to J.I.M. We are indebted to Dr. Anne-Marie Levelut (Université Paris-Sud) for kindly providing access to the equipment for the X-ray study of oriented samples.

---

(29) Martínez, J. I.; Alonso, P. J.; Orera, V. M. *Proc 3rd Int. Sym. Metallomesogens*; Peñiscola, Spain, June, 1993.